

# Dynamics of Photo-excited Spins in InSb Based Quantum Wells

K. Nontapot, R. N. Kini, B. Spencer, G. A. Khodaparast\*  
*Department of Physics, Virginia Tech, Blacksburg, VA 24061*

N. Goel, S. J. Chung, T. D. Mishima and, M. B. Santos  
*Homer L. Dodge Department of Physics and Astronomy, University of Oklahoma, Norman, OK, 73019*  
(Dated: October 23, 2018)

We report time resolved measurements of spin relaxation in doped and undoped InSb quantum wells using degenerate and two-color magneto-optical Kerr effect techniques. We observed that the photo-excited spin dynamics are strongly influenced by laser excitation fluence and the doping profile of the samples. In the low fluence regime, an oscillatory pattern was observed at low temperatures ( $\leq 77$  K) in the samples with an asymmetric doping profile which might be attributed to the quasi-collision-free spin relaxation regime. Our measurements also suggest the influence of the barrier materials ( $\text{Al}_x\text{In}_{1-x}\text{Sb}$ ) on the spin relaxation in these material systems.

PACS numbers: 75.50.Pp, 78.20.Ls, 78.47.+p, 78.66.Fd

## 1. INTRODUCTION

In light of the growing interest in spin-related phenomena and devices, there is now a renewed interest in the science and engineering of narrow gap semiconductors (NGS) such as InSb. NGS offer several scientifically unique electronic features such as a small effective mass, a large g-factor, a high intrinsic mobility, and large spin-orbit coupling effects. In semiconductors with large spin-orbit interaction the coupling of electron spin polarization with electric fields or currents can provide new opportunities for spin manipulation in both electronic and optoelectronic devices. In particular, spin splitting in heterostructures caused by bulk inversion asymmetry (BIA) [1] and structural inversion asymmetry (SIA), often called Rashba splitting [2, 3] has attracted much attention and understanding various properties and interactions in these heterostructures is important. Several recent transport measurements have demonstrated mesoscopic spin-dependent ballistic transport in InSb-based heterostructures [4, 5]. In addition, the integration of InSb quantum well (QW) transistors onto silicon substrates has been investigated recently [6]. The performance of field effect transistors (FETs) suitable for digital logic circuits was demonstrated on material with a buffer just  $1.8 \mu\text{m}$  thick which is an initial step towards integrating InSb FETs with Si CMOS for high-speed, energy-efficient logic applications [7].

In bulk n-type semiconductors, two spin relaxation mechanisms, the Dyakonov-Perel (DP) [8] and Elliot-Yaffet (EY) [9] are known to be the dominant relaxation processes. The EY relaxation process originates from strong mixing of the valence band states and conduction bands in NGS resulting in non-zero transition rates even for spin-conserving scattering process. For QWs, the spin

relaxation rate,  $\tau_s$ , in the frame of EY process is modeled as following: [10]

$$\frac{1}{\tau_s^{EY}} = C_{EY} \eta^2 \left(1 - \frac{m_e}{m_0}\right)^2 \frac{E_{1e}}{E_g^2} k_B T \frac{1}{\tau_p}, \quad (1)$$

where  $\eta = \frac{\Delta}{E_g + \Delta}$ ,  $\Delta$  is the spin-orbit splitting of the valence band,  $m_e/m_0$  is the electron effective mass ratio,  $E_{1e}$  is the confinement energy for the lowest electron sub-band,  $E_g$  is the band gap,  $\tau_p$  is the momentum relaxation time and  $C_{EY}$  is a dimensionless constant predicted to be nearly unity [10].

In DP mechanism, the lack of inversion symmetry in the presence of a k-dependent spin-orbit interaction can lift the spin degeneracy even in the absence of an external magnetic field. In the DP picture, the spin relaxation rate for QWs is given by [10, 11],

$$\frac{1}{\tau_s^{DP}} = C_{DP} \frac{\alpha^2}{2} \frac{E_{1e}^2}{\hbar^2 E_g} k_B T \tau_p, \quad (2)$$

where  $C_{DP}$  is a dimensionless constant predicted to be 16 [10, 11] and  $\alpha$  is a parameter characterizing the  $k^3$  term for conduction band electrons given by:

$$\alpha \approx \frac{4\eta}{(3-\eta)^{1/2}} \frac{m_e}{m_0} \quad (3)$$

In the case of the DP process, it would be possible to alter the spin lifetime with an applied electric field which can modulate the strength of the spin-orbit coupling via the Rashba effect. In addition, changing the momentum relaxation time can modulate the spin relaxation time in both the EY and the DP mechanisms.

In a recent report, the temperature and mobility dependences of the spin relaxation time in Te-doped InSb/ $\text{Al}_{0.15}\text{In}_{0.85}\text{Sb}$  QWs have been probed suggesting a fast spin relaxation time of 0.5 ps [12]. The anti-localization measurements of the InSb-based QWs studied in this work have suggested  $\tau_s \sim 12$  ps at temperatures below 10 K [13]. Here we report the dynamics

\*Author to whom correspondence should be addressed; Electronic address: khoda@vt.edu

of photo-excited spins in several InSb based QWs using magneto-optical Kerr effect (MOKE) spectroscopy.

## 2. SAMPLES

We probed relaxation of photo-excited spins in the  $\text{Al}_x\text{In}_{1-x}\text{Sb}/\text{InSb}$  QW structures in several optical excitation regimes. In the first regime the pump/probe pulses were from a single NIR tunable laser with a maximum fluence of  $50 \mu\text{J cm}^{-2}$  on the samples. In the second regime, the pump excitation was tuned in the mid infrared (MIR) region with a maximum fluence of  $10 \text{ mJ cm}^{-2}$  with the probe fixed at 800 nm. We observed that the photo-excited spin dynamics are strongly influenced by excitation wavelength, laser fluence, and samples' growth profiles. Our results are important to develop concepts toward development of devices employing InSb based heterostructures and to understand the effect of spin-orbit coupling in the relaxation dynamics in NGS. Our InSb square single quantum wells (QWs) were grown on GaAs (001) substrates by MBE at the University of Oklahoma. The  $\text{Al}_x\text{In}_{1-x}\text{Sb}$  barrier layers are  $\delta$ -doped with Si. The layers are located either on one side of the QW (asymmetric sample) or equidistant on both sides of the QW (symmetric sample). The  $\delta$  doped layers within the barrier layers are typically located 70 nm from the well center. The shape and symmetry of the wells is expected to be determined by whether one or both barriers are doped. We studied an undoped and five remotely  $\delta$ -doped InSb QWs with the electron concentrations in the wells ranging from  $\sim 1 - 4.4 \times 10^{11} \text{ cm}^{-2}$ , where only the ground-state subband is occupied and the mobility is in the range  $\sim 70,000 - 100,000 \text{ cm}^2/\text{Vs}$  at 4.2 K. Detailed growth conditions were described previously [14, 15]. The characteristics of the samples are summarized in Table I, where samples S1, S2, S3, A1 and A2 are single modulation doped QWs and M1 is an undoped multi-QW (MQW) structure with 24 wells separated by 50 nm  $\text{Al}_x\text{In}_{1-x}\text{Sb}$  barriers.

TABLE I: *Characteristics of the samples studied in this work. The densities and mobilities are from the measurements at 4.2 K. In the doped samples, only the first subband is occupied and the Fermi levels,  $E_F$ , are with respect to the bottom of conduction band.*

Sample	Density $\text{cm}^{-2}$	Mobility $\text{cm}^2/\text{Vs}$	QW Width nm	$x$ %	CB1 meV	$E_F$ meV
S1(S769)	$2.0 \times 10^{11}$	100,000	30	9	14.4	33
S2(S499)	$1.8 \times 10^{11}$	135,000	30	9	14.4	29
S3(S939)	$4.4 \times 10^{11}$	96,000	11.5	15	53	72
A1(S360)	$2.2 \times 10^{11}$	73,000	30	9	14.4	36
A2(S206)	$1.0 \times 10^{11}$	70,000	30	7	13.6	16
M1(S591)	Undoped		30	9		

The band offsets in this system has been determined earlier [16]. To calculate the interband transition ener-

gies we have used a four-band model described by Bastard [17] with band-edge masses of  $0.0139m_0$ ,  $0.015m_0$ , and  $0.25m_0$  for the electrons, light holes, and heavy holes, respectively, where  $m_0$  is the free electron mass. The results of the calculations for the interband transitions in our samples at 4.2 K are summarized in Table II. Band-edge effective mass values in the alloy barrier are considered to change with the band gap  $E_g^x$  according to the Kane [18] model. The energy gap (in eV) of the alloy at 4.2 K can be calculated from the known variation of the alloy gap with concentration  $x$ :  $E_g^x = E_g^0 + 2.06x$  [19]. In addition, the effect of strain has been included in determination,  $E_g^0$ , the band gap of the InSb QWs [20]. The variation in the bandgap of both InSb and  $\text{Al}_x\text{In}_{1-x}\text{Sb}$  below 77 K is about 3% [19] resulting in no significant variation in the 2D confinement potentials and the interband transition energies.

TABLE II: *Calculated possible interband transition energies for the samples with different alloy concentrations and well widths at 4.2 K.*

Alloy %	Well Width nm	CB1-HH1 meV( $\mu\text{m}$ )	CB2-HH2 meV( $\mu\text{m}$ )	CB1-LH1 meV( $\mu\text{m}$ )	CB2-LH2 meV( $\mu\text{m}$ )
7	30	261(4.7)	300(4.1)	291(4.26)	343(3.6)
9	30	265(4.68)	330(3.75)	302(4.1)	360(3.45)
15	11.5	318(3.9)	449 (2.76)	386(3.2)	NA

## 3. EXPERIMENTAL TECHNIQUE

We probed photo-excited spins in the  $\text{Al}_x\text{In}_{1-x}\text{Sb}/\text{InSb}$  QW structures at two optical excitation regimes. The experimental details of these two regimes are described in this section. Both degenerate and two-color pump-probe techniques were employed to study the spin relaxations. The degenerate pump-probe experiments were performed using a mode-locked Ti:Sapphire laser which produces tunable radiation from 750 to 850 nm with a repetition rate of 80 MHz, with a maximum fluence of  $50 \mu\text{J cm}^{-2}$  on the samples. A small portion ( $\approx 10\%$ ) of the laser beam was split off to be used as the probe. The pump beam was modulated at frequency of 1 KHz with a mechanical chopper. In this configuration, the excitation laser can not avoid exciting carriers in the  $\text{Al}_x\text{In}_{1-x}\text{Sb}$  barrier layer. Our earlier time resolved cyclotron resonance measurements on an undoped InSb MQW demonstrated that exciting the sample with 800 nm pulses can result in high density of photo-excited carriers in the wells [21].

Our two-color pump-probe measurements were performed using an optical parametric amplifier (OPA) excited by a Ti:Sapphire chirped pulse amplifier (CPA) with a repetition rate of 1 KHz. The OPA beam was used as the MIR pump, with a maximum fluence of  $10 \text{ mJ cm}^{-2}$  on the samples and a small portion of the CPA

( $10^{-5}$ ) was used as the probe. In these measurements the pump excitation created carriers in the barrier layer except when the sample S3 was pumped at a wavelength of  $2.6 \mu\text{m}$ .

As a result of selection rules for interband transitions, spin-polarized carriers can be created using circularly polarized pump beams. The MOKE signal arises from the difference between the optical coefficients of a material for left and right circularly polarized light which is proportional to the magnetization  $M$  [22].

$$\eta_k + i\theta_k = -(\kappa^+ - \kappa^-)/(2n(n^2 - 1)) \quad (4)$$

where  $\theta_k$  is the Kerr rotation,  $\eta_k$  is the Kerr ellipticity,  $n$  is the index of refraction, and  $\kappa^+$  and  $\kappa^-$  are the optical susceptibilities of the material for right ( $\sigma^+$ ) and left ( $\sigma^-$ ) circularly polarized light, respectively. Since  $(\kappa^+ - \kappa^-) \propto M$ , the MOKE effect can be induced by an external magnetic field, or an optically or a spontaneous induced magnetization [22]. Using a Wollaston prism, the reflected NIR signal was separated into s- and p- components which are orthogonal and have equal intensity in the equilibrium spin density state. In the presence of non-equilibrium spin polarized carriers, the MOKE signal reflects as an intensity difference between the s- and p- components of the reflected probe pulses. The signals were monitored using a Si balanced detector and were fed into a lock-in amplifier.

#### 4. RESULTS AND DISCUSSION

Here we report the results of MOKE induced by optical magnetization to measure spin relaxations. Temporal traces of time resolved MOKE for the sample A1 at 77 K for  $\sigma^+$ ,  $\sigma^-$ , and linearly polarized lights are shown in Fig. 1. The measurements were taken under the excitation by NIR radiation at 775 nm with average power  $\sim 400$  mW (fluence of  $\sim 50 \mu\text{J}\cdot\text{cm}^{-2}$ ) resulting in a photo-induced carrier density of  $\sim 5 \times 10^{17} \text{cm}^{-3}$ . As shown for  $\sigma^+$ , at timing zero, sample A1 demonstrates a sharp increase in the MOKE signal followed by a rapid recovery of the signal. The same measurement for  $\sigma^-$  shows a similar pattern which is not a mirror image of the trace shown for  $\sigma^+$ . No residual MOKE signal was observed for the linear polarization of the pump. The inset shows the MOKE signal at 4.2 K for  $\sigma^+$  which exhibits the same oscillatory pattern. As shown in Fig. 2a for sample A2, under similar experimental conditions, we observed oscillations at 77 K. The oscillations appear at time delays greater than 10 ps and do not appear at negative time delays. The oscillatory pattern can be attributed to precession of  $z$  components of electron spins at the Fermi level with possible contributions from both BIA and SIA. A similar damped oscillatory behavior has been observed in a high-mobility n-doped GaAs/AlGaAs at temperatures below 5 K [23, 24]. This effect has been attributed to the breakdown of collision-dominated regime of spin

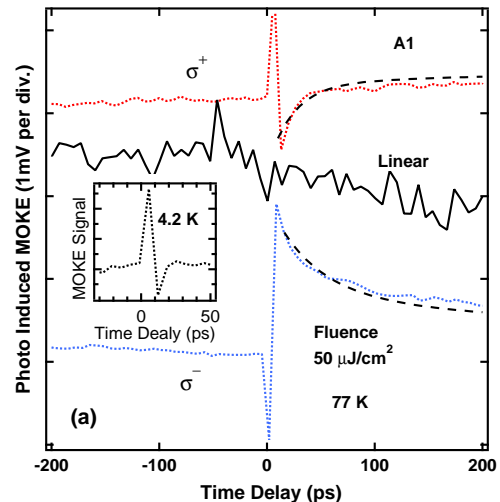


FIG. 1: Photo-induced MOKE of sample A1 at 77 K versus time delay under pumping with circularly and linearly polarized radiations at 775 nm and probing with the same wavelength. The upper trace represents the photo-induced carrier density. The laser fluence is estimated to be in the order of  $50 \mu\text{J}\cdot\text{cm}^{-2}$ . The inset shows the MOKE measurement for one pump polarization at 4.2 K. The dashed lines represent exponential fits to the data and for clarity are shifted slightly.

relaxation. In their case, the SIA considered to be 10 times less important than the BIA.

In our case, the calculated potential profile of the conduction band in a 30 nm wide asymmetric InSb/Al<sub>0.09</sub>In<sub>0.91</sub>Sb QW with doping density of  $\sim 2.0 \times 10^{11} \text{cm}^{-2}$  suggests an in built electric field of  $3.3 \times 10^6 \text{V/m}$  corresponding to an effective magnetic field of  $\sim 0.3 \text{mT}$  [25]. In our samples, the damped oscillations occur at higher temperatures (77 K or lower) compared to the GaAs/AlGaAs structures [23, 24]. If our observed oscillations are due to the spin precession at zero applied magnetic field, then InSb QWs are potentially useful in spin FETs that operate at higher temperatures. If we only include the spin-polarized photo-induced carriers, with a density on the order of  $5.0 \times 10^9 \text{cm}^{-2}$ , we obtain oscillation frequency,  $\Omega_{(K_F)}$ , at the Fermi level equal to 0.7 rad/ps corresponding to a period of  $\sim 9$  ps. In this scenario, the calculated frequency is the same order of magnitude as the observed oscillation frequency in our measurements. The  $\Omega_{(K_F)}$  and the period change to 4 rad/ps and 1.5 ps, respectively, if we include a total density of  $2.0 \times 10^{11} \text{cm}^{-2}$ . In these estimations, the Rashba splitting strength of  $\alpha_R = 1.3 \times 10^{-9} \text{eV}\cdot\text{cm}$  was used [15]. Using  $\alpha_R = 1 \times 10^{-10} \text{eV}\cdot\text{cm}$  with a total density of  $2.0 \times 10^{11} \text{cm}^{-2}$  results in  $\Omega_{(K_F)}$  of 0.3 rad/ps, closer to the observed frequency in our measurements. This smaller order of magnitude for  $\alpha_R$  has been calculated for a well width of 30 nm and electron density of  $2.0 \times 10^{11} \text{cm}^{-2}$  in Ref. [26]. Recently the Larmor frequency of bulk InSb has been measured suggesting a

spin precession period of 5-10 ps, depending on the laser pumping wavelength [27].

If the product of  $\Omega_{(K_F)}\tau_p \geq 1$ , spins precess more than a full cycle before being scattered. On the other hand if this product is smaller than 1, the individual electron spin can only precess by some fraction of a full cycle before the momentum scattering changes the amplitude and direction of the effective magnetic field [23, 24]. In our case for the measured  $\Omega_{(K_F)} = 0.2$  rad/ps, if we use the value of the momentum scattering,  $\sim 0.6$  ps, from the measured Hall mobility at 77 K, a collision-free condition would not be satisfied unless the momentum scattering time of the photo-induced spin polarized carriers is significantly larger than the value obtained from the Hall mobility ( $\sim 0.6$  ps) for the electrons already in the QW. In the following sections the results of our measurements in symmetric samples are presented.

Figure 2b demonstrates the typical spin relaxations in the symmetric samples S1, S2, and the MWQ, M1. For a fluence of about  $50 \mu\text{J}\cdot\text{cm}^{-2}$  the relaxations in S1, S2 and M1 exhibit some similar patterns. If we refer to the relaxation time as the time when the signal at positive time delay reaches approximately to the same value the negative time delay. The temperature dependence of relaxations in these structure is rather weak but as shown for S2, the relaxation time is slightly tunable as a function of the laser fluence. The lack of oscillations in the MOKE signal of our symmetric samples could suggest that the BIA is not a dominant mechanism of the spin splitting in these structures. It has been suggested and probed by several groups that BIA dominates mainly in large gap semiconductors [28, 29, 30, 31].

In the second regime probed by our measurements, we used a two-color MOKE scheme, using MIR pump pulses fixed at  $2 \mu\text{m}$  and NIR probe pulses fixed at 800 nm. For the samples studied here  $2 \mu\text{m}$  (620 meV) pump pulses can not avoid exciting the carriers in the  $\text{Al}_x\text{In}_{1-x}\text{Sb}$  barrier layers, but the significance of this scheme was that it allowed probing the relaxations at a higher fluence compared to the degenerate regime. Examples of the measurements are shown in Fig. 3a and 3b for two different samples (A1 and S1) at RT. In this regime the photo-induced spin relaxations show exponential decays faster by an order of magnitude compared to the lower fluence regimes shown in Fig 2. This can be explained using the EY mechanism where the spin relaxation time is directly proportional to momentum scattering time. At higher excitation fluences the momentum scattering time is expected to be shorter (due to the existence of high photo-induced carrier density) and the observation of a faster spin relaxation is expected for the EY mechanism.

Figure 3c shows the spin relaxation traces for the sample S3 at several temperatures in the high fluence regime. Compared to the samples A1 and S1, the sample S3 shows a longer spin relaxation time in the high fluence regime. In the case of S3, using  $2.6 \mu\text{m}$  radiation (477 meV, this photon energy is close to the HH2-CB2 transi-

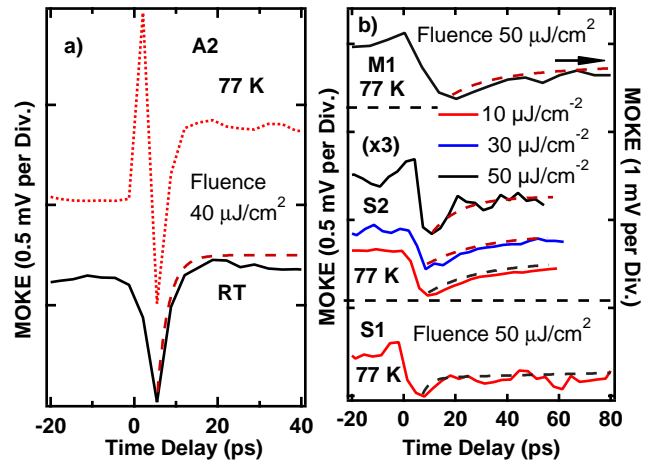


FIG. 2: a) Photo-induced MOKE of sample A2 at 77 K and room temperature (RT) versus time delay. Multi-step relaxation disappears at temperatures above 77 K and the temperature dependence above 77 K is weak. b) Top trace: MOKE of the undoped sample, M1, at 77 K for fluence of  $\sim 50 \mu\text{J}\cdot\text{cm}^{-2}$ . Middle traces: MOKE traces of the sample S2 at different laser fluences, . Lower trace: MOKE signals in the sample S1 for a fluence  $\sim 50 \mu\text{J}\cdot\text{cm}^{-2}$ . In the samples S1, S2, and M1 the temperature dependence is weak and data is shown only for the measurements at 77 K. The dashed lines represent exponential fits to the data and for clarity are shifted slightly.

tion in this sample) for the pump, it is possible to excite carriers only in the InSb well and not in the  $\text{Al}_{0.15}\text{In}_{0.85}\text{Sb}$  barrier layer. This fact is supported by earlier measurements that determined the concentration and temperature dependence of the fundamental energy gap in  $\text{Al}_x\text{In}_{1-x}\text{Sb}$  [19]. In addition, as shown recently for bulk InSb at RT [32], a large density of photoholes can reduce the momentum relaxation time, ( $\tau_p$ ), of the electrons and therefore if the DP process is dominant, an increase in the spin lifetime can be observed. In bulk n-InSb this effect was found to increase the spin lifetime by a factor of 2 to 3, changing the spin relaxation from 14 to 38 ps. As shown in Fig. 3c at 77 K for several laser fluences, we observe modification of the relaxation patterns by the density of photo-induced carriers. The effect of pump fluence and therefore initial spin polarization in a high mobility GaAs/AlGaAs single QW has been probed, suggesting a similar increase in spin relaxation time by increasing the initial spin polarization [24]. In our samples, we only see this effect when we selectively pump the InSb well layer and avoid the barrier materials.

In general, we believe that some of the observed differences could be also due to the differences in the growth profiles. For example, S3 (the 11.5 wide QW) has 13 nm of InSb cap layer and 139.5 nm of  $\text{Al}_x\text{In}_{1-x}\text{Sb}$  layer above the well, whereas the 30 nm QWs, except S2, has a 10 nm thick InSb cap layer. S2 has a 20 nm thick InSb cap layer. In addition, samples A1, A2, S1 and S2 have

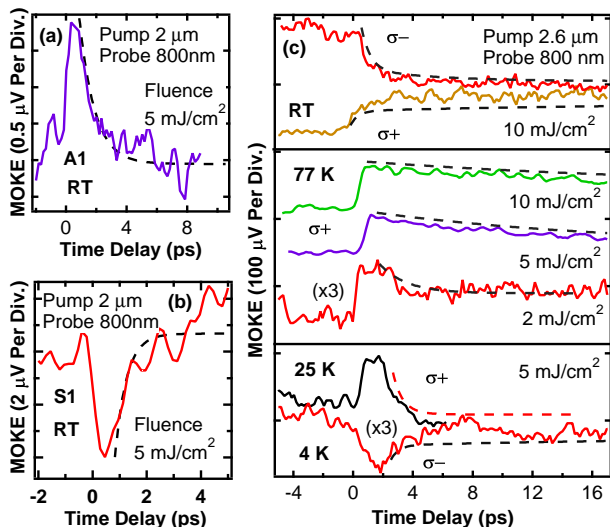


FIG. 3: a) and b) show examples of the two-color MOKE measurements in high fluence regime. c) MOKE traces of sample S3 at different laser fluences and temperatures. At RT we were able to observe MOKE at the highest available fluence ( $10 \text{ mJ}\cdot\text{cm}^{-2}$ ) where the relaxations show a step pattern rather than an exponential decay. The dashed lines represent exponential fits to the data and for clarity are shifted slightly.

25 nm, 60 nm, 170 nm and 130 nm of  $\text{Al}_x\text{In}_{1-x}\text{Sb}$  above the InSb QW layers, respectively. Sample M1 which is a MQW, has a 10 nm thick InSb cap layer with 50 nm thick barriers above and below each well. The absorption length in these heterostructures (in the wavelength region used in this study) is about  $0.5 \mu\text{m}$ ; therefore, the regions where the photo-generated carriers are created can be different in each sample. In our measurements, the best case to compare the experimental data with the DP and EY models, is the case in Fig. 3c. In this sample (S3) using  $2.6 \mu\text{m}$ , we have avoided the barrier material. Using the momentum scattering time from the measured Hall mobility, the calculated spin relaxation,  $\tau_s$ , according to the EY and DP models are summarized in Table III. It has been theoretically predicted that for III-V bulk semiconductors, EY mechanism is dominant at very low temperatures ( $T < 6 \text{ K}$ ) [33]. However, it has been reported that a cross-over to the DP mechanism can occur even at RT in low mobility ( $\sim 10,000 \text{ cm}^2/\text{Vs}$ ) InSb QW samples [34]. In our case the EY model provides a better fit for the RT observation and the DP for the measurements at 4.2 K.

## 5. CONCLUSIONS

We report spin relaxation measurements in a series of InSb based QWs. In the low fluence regime ( $\sim 50 \mu\text{J}\cdot\text{cm}^{-2}$ ), an oscillatory pattern was observed in samples with asymmetric doping profiles at low temperatures ( $\leq 77\text{K}$ ) which can be attributed to a quasi-collision-free

TABLE III: Calculated spin relaxation times  $\tau_s$  with  $C_{DP} = 16$  and  $C_{EY} = 1$  for sample S3 using Eq. 1 and Eq. 2, compared to the experimental observations at several temperatures with a significant variation in the relaxation times.

Sample	T(K)	$\tau_s(DP)$ (ps) theory	$\tau_s(EY)$ (ps) theory	$\tau_s$ (ps) experiment
S3	4.2	7	3827	$\sim 8$
	25	1.3	535	$\sim 6$
	77	0.6	124	$> 16$
	300	0.4	12	$\gg 16$

spin relaxation regime. Probing this effect further by gating the samples or by adjusting the asymmetric doping level to alter the built-in electric field and therefore tuning the effective magnetic field, can provide more insight to this observation. In addition, the actual value of  $\alpha_R$  (the SIA factor or the Rashba coefficient) which controls the precession frequency of the photoexcited carriers is a crucial factor to model the observations. In a high fluence regime, using a two-color setup and not avoiding the barrier materials, we observed faster spin relaxations expected from the EY mechanism. By selectively pumping the well of sample S3, we observed spin relaxation times which were different from non-selective pumping schemes. This fact might suggest that the spin relaxation observed in the non-selective pumping can be influenced by the barrier materials. We will be extending our measurements to probe samples with higher alloy concentrations when they become available and to probe the spin relaxations using the differential transmission technique in MIR.

**Acknowledgment:** This work has been supported by NSF-DMR-0507866, Jeffress-J748, Advance-VT, AFOSR Young Investigator Program-06NE231, NSF-DMR-0510056 and DMR-0520550.

- 
- [1] G. F. Dresselhaus, Phys. Rev. **100**, 580 (1955).
- [2] Y.A. Bychkov and E.I. Rashba, J. Phys. C **17**, 6039 (1984); Y.A. Bychkov and E.E. Rashba, Pis'ma Zh. Eksp. Teor. Fiz. **39**, 66 (1984) [JETP Lett. **39**, 78 (1984)].
- [3] E.I. Rashba, Fiz. Tverd. Tela (Leningrad) **2**, 1224 (1960) [Sov. Phys.-Solid State **2**, 1109 (1960)]; E.I. Rashba and V.I. Sheka in Landau Level Spectroscopy, Modern Problems in Condensed Matter Sciences, Vol. 27.1 (North-Holland, Amsterdam, 1991) pp. 132-206.
- [4] Hong Chen, J. J. Heremans, J. A. Peters, N. Goel, S. J. Chung, and M. B. Santos, Appl. Phys. Lett. **86**, 032113 (2005).
- [5] A. R. Dedigama, D. Deen, S. Q. Murphy, N. Goel, J. Keay, M. B. Santos, K. Suzuki, S. Miyashita, and Y. Hirayama, Physica E **34**, 647 (2006).
- [6] T. Ashley, L. Buckle, S. Datta, M. T. Emeny, D. G. Hayes, K. P. Hilton, R. Jefferies, T. Martin, T. J. Phillips, D. J. Wallis, P. J. Wilding, R. Chan R, ELECTRONICS LETTERS **43**(14), 777-779 (2007).
- [7] J. M. S. Orr, P. D. Buckle, M. Fearn, C J Storey, L. Buckle, and T. Ashley, New Journal of Physics **9** 262 (2007).
- [8] M. I. D'yakonov and V. I. Perel, Sov. Phys. JETP **33**, 1053 (1971); Sov. Phys. Solid State **13**, 3023 (1972).
- [9] R. J. Elliott, Phys. Rev. **96**, 266 (1954); Y. Yafet, Solid State Physics, edited by F. Seitz and D. Turnbull Academic, New York, (1963), Vol. 14.
- [10] Tackeuchi A, Kuroda T, Muto S, Nishikawa Y and Wada O 1999 Japan. J. Appl. Phys. **38** 4680(1999).
- [11] Tackeuchi A, Wada O and Nishikawa Y Appl. Phys. Lett. **70** 1131(1997).
- [12] K. L. Litvinenko, B. N. Murdin, J. Allam, C. R. Pidgeon, M. Bird, K. Morris, W. Branford, S. K. Clowes, L. F. Cohen, T. Ashley and L. Buckle, New Journal of Physics, **8**, 49 (2006).
- [13] Private communications with J. J. Heremans.
- [14] K. J. Goldammer, W. K. Liu, G. A. Khodaparast, S. C. Lindstrom, M. B. Johnson, R. E. Doezema, M. B. Santos J. Vac. Sci. Technol. **B16**, 1367 (1998).
- [15] G. A. Khodaparast, R. E. Doezema, S. J. Chung, K. J. Goldammer, and M. B. Santos Phys. Rev. B **70**, 155322 (2004).
- [16] N. Dai, G. A. Khodaparast, F. Brown, R. E. Doezema, S. J. Chung, and M. B. Santos, Appl. Phys. Lett. **76**, 3905 (1998).
- [17] G. Bastard, Wave Mechanics Applied to Semiconductor Heterostructures (Les Editions Physique, Les Ulis, 1988).
- [18] E. O. Kane, J. Phys. Chem. Solids **1**, 249 (1957); in Handbook on Semiconductors, edited by W. Paul North-Holland, Amsterdam, 1982, Vol. 1, p. 193.
- [19] N. Dai, F. Brown, R. E. Doezema, S. J. Chung, K. J. Goldammer, and M. B. Santos, Appl. Phys. Lett., **73**, 3132 (1998).
- [20] N. Dai, F. Brown, P. Barsic, G. A. Khodaparast, R. E. Doezema, M. B. Johnson, S. J. Chung, K. J. Goldammer, and M. B. Santos **73**, 1101 (1998).
- [21] G. A. Khodaparast, D. C. Larrabee, J. Kono, D. S. King, S. J. Chung, and M. B. Santos, Phys. Rev. B **67**, 035307 (2003).
- [22] A. K. Zvezdin and V. A. Kotov, *Modern Magneto-optics and Magneto-optical Materials* (IoP Publishing, Bristol, 1997).
- [23] M. A. Brand, A. Malinowski, O. Z. Karimov, P. A. Marsden, and R. T. Harley, A. J. Shields and D. Sanvitto, D. A. Ritchie and M.Y. Simmons, Phys. Rev. Lett, **89**,236601 (2002).
- [24] D. Stich, J. Zhou, T. Korn, R. Schulz, D. Schuh, W. Wegscheider, M. W. Wu, and C. Schüller, Phys. Rev. B **76**, 205301 (2007).
- [25] P. Pfeffer and W. Zawadzki, Phys. Rev. B **68**, 035315 (2003).
- [26] A. M. Gilbertson, M. Fearn, J. H. Jefferson, B. N. Murdin, P. D. Buckle, and L. F. Cohen, Phys. Rev. B **77**,165335 (2008).
- [27] K. L. Litvinenko, L. Nikzad, C. R. Pidgeon, J. Allam, L. F. Cohen, T. Ashley, M. Emeny, W. Zawadzki, and B. N. Murdin, Phys. Rev. B **77**, 033204 (2008).
- [28] G. Lommer, F. Malcher, U. Rössler, Phys. Rev. B **60**, 728 (1988).
- [29] P. Pfeffer and W. Zawadzki, Phys. Rev. B **68**, 035315 (2003).
- [30] W. Zawadzki and P. Pfeffer, Semicond. Sci. Technol. **19**, R1 (2004).
- [31] P. Pfeffer and W. Zawadzki, Phys. Rev. B **59**, R5312 (1999).
- [32] B. N. Murdin, K. Litvinenko, and D. G. Clarke, C. R. Pidgeon and P. Murzyn, P. J. Phillips, D. Carder, G. Berden, B. Redlich, A. F. G. van der Meer, S. Clowes, J. J. Harris, L. F. Cohen Blackett, T. Ashley, L. Buckle, Phys. Rev. Lett. **96**, 096603 (2006).
- [33] P. H. Song and K. W. Kim, Phys. Rev. B **66**, 035207 (2002).
- [34] K. L. Litvinenko, B. N. Murdin, J. Allam, C. R. Pidgeon, M. Bird, K. Morris, W. Branford, S. K. Clowes, L. F. Cohen, T. Ashley and L. Buckle, New Journal of Physics, **8**, 491 (2006).